*Inorg. Chem.* **2007**, *46*, 10307–10311


# A Shape-Controlled Method to Functionalize Multiwalled Carbon Nanotubes with $Ni_3S_2$

**Ji Min Du and Dae Joon Kang***

*BK 21 Physics Research Division, Institute of Basic Science, SKKU Advanced Institute of Nanotechnology and Center for Nanotubes and Nanostructured Composites, Sungkyunkwan University, Suwon 440-746, Republic of Korea*

Received May 15, 2007

In this paper, we report the funtionalization of multiwalled carbon nanotubes (MWCNTs) with $Ni_3S_2$ using a solvent–thermal approach. The nanocomposites synthesized without ammonia show that the MWCNTs' outer surface was uniformly coated with a $Ni_3S_2$ film appearing like centipede-shaped objects when characterized by scanning transmission electron microscopy and transmission electron microscopy images. Meanwhile, the $Ni_3S_2$ layer thickness can be changed by simply altering the concentration of reaction precursors and keeping the other reaction conditions constant. Interestingly, clustered $Ni_3S_2$ nanoparticles were formed along the outside surfaces of the MWCNTs when ammonia was added to the reaction solution while keeping all other conditions unchanged. Also, the sizes of $Ni_3S_2$ nanoparticles can be varied through varying the amount of ammonia in our reaction system. On the basis of our experimental results, we propose a dynamic-controlled Oswald ripening mechanism to elucidate the formation of the MWCNTs composites with centipede-shaped and clustered $Ni_3S_2$ morphologies.

## 1. Introduction

Since the discovery of carbon nanotubes (CNTs),[1] they have been widely investigated owing to their unique electronic and catalytic properties, one-dimension morphology, and relative stability, making them exhibit many potential applications in electronic devices,[2] gas sensors,[3] catalytic reactions,[4] and so on.[5] Moreover, CNTs also offer an excellent platform for functionalizing with other compounds to develop unprecedented properties. Therefore, much effort has been spent in modifying CNTs with polymers and inorganic and organic complexes over the past several years.[6] In general, to date there are two methods of covalent and noncovalent interaction employed to modify CNTs.[7] The covalent linkage ability of CNTs is for the formation of chemical bonds between the CNTs surface and functional groups such as carboxylic acids, amines, etc.[8] On the other hand, the noncovalent functionalization of CNTs utilizes $\pi$ stacking, van der Waals, as well as electronic interactions between functional compounds and the CNT surfaces.[9] Recently, noncovalent functionalization for CNTs has received more attention since functionalized CNTs not only can preserve nearly all the properties of the pristine CNTs but also result in better electrical conductivity,[10] enhanced optical properties,[11] and higher Young's modulus values.[12]

* To whom correspondence should be addressed. E-mail: djkang@skku.edu.Tel: +82-(0)31-290-5906. Fax +82-(0)31-290-5947.

(1) Iijima, S. *Nature* **1991**, *354*, 56.
(2) Maehashi, K.; Ozaki, H.; Ohno, Y.; Inoue, K.; Matsumoto, K.; Seki, S.; Tagawa, S. *Appl. Phys. Lett.* **2007**, *90*, 023103.
(3) Kong, J.; Chapline, M. G.; Dai, H. *Adv. Mater.* **2001**, *13*, 1854.
(4) Wildgoose, G. G.; Banks, C. E.; Compton, R. G. *Small* **2006**, *2*, 182.
(5) Ouyang, M.; Huang, J. L.; Cheung, C. L.; Lieber, C. M. *Science* **2001**, *292*, 702.
(6) (a) Kong, J.; Franklin, N. R.; Zhou, C.; Chaplin, M. G.; Peng, S.; Cho, K.; Dai, H. *Science* **2000**, *287*, 622. (b) Tans, S. J.; Verschueren, R. M.; Dekker, C. *Nature* **1998**, *393*, 49. (c) Liu, Z.; Shen, Z.; Zhu, T.; Hou, S.; Ying, L.; Shi, Z.; Gu, Z. *Langmuir* **2000**, *16*, 3569. (d) Unger, E.; Graham, A.; Kreupl, F.; Liebau, M.; Hoenlein, M. *Curr. Appl. Phys.* **2002**, *2*, 107. (e) Nakashima, N.; Tomonari, Y.; Murakami, H. *Chem. Lett.* **2002**, *6*, 638.
(7) (a) Hirsch, A. *Angew. Chem.* **2002**, *41*, 1853. (b) Sotiropoulou, S.; Chaniotakis, N. A. *Anal. Bioanal. Chem.* **2003**, *375*, 103. (c) Chen, J.; Hamon, M. A.; Hu, H.; Chen, Y.; Rao, A. M.; Eklund, P. C.; Haddon, R. C. *Science* **1998**, *282*, 95. (d) Raghuveer, M. S.; Agrawal, S.; Bishop, N.; Ramanath, G. *Chem. Mater.* **2006**, *18*, 1390.
(8) (a) Holzinger, M.; Vostrowsky, O.; Hirsch, A.; Hennrich, F.; Kappes, M.; Weiss, R.; Jellen, F. *Angew. Chem.* **2001**, *113*, 4132. (b) Liu, L.; Wang, T.; Li, J.; Guo, Z. X.; Dai, L.; Zhang, D.; Zhu, D. *Chem. Phys. Lett.* **2003**, *367*, 747. (c) Holzinger, M.; Abraham, J.; Whelan, P.; Graupner, R.; Ley, L.; Hennrich, F.; Kappes, M.; Hirsch, A. *J. Am. Chem. Soc.* **2003**, *125*, 8566. (d) Holzinger, M.; Vostrowsky, O.; Hirsch, A.; Hennrich, F.; Kappes, M.; Weiss, R.; Jellen, F. *Angew. Chem., Int. Ed.* **2001**, *40*, 4002. (e) Ni, B.; Sinnott, S. B. *Phys. Rev. B: Condens. Matter Mater. Phys.* **2000**, *61*, 16343.
(9) (a) Cheng, F.; Adronov, A. *Chem.—Eur. J.* **2006**, *12*, 5053. (b) Zurek, E.; Autschbach, J. *J. Am. Chem. Soc.* **2004**, *126*, 13079.
(10) Moriguchi, I.; Hidaka, R.; Yamada, H.; Kudo, T.; Murakami, H.; Nakashima, N. *Adv. Mater.* **2006**, *18*, 69.
(11) Brady, R.; Flynn, B. R.; Geoffroy, G. L.; Gray, H. B.; Peone, J. J.; Vaska, L. *Inorg. Chem.* **1976**, *15*, 1485.

10.1021/ic700936c CCC: $37.00 
Published on Web 11/01/2007

More recently, these functionalized CNTs have been exploited as rectifying diodes,[13] detection media for cancer,[14] and a vehicle of drug delivery.[15] For example, Wu et al. utilized functionalized CNTs to deliver amphotericin B to cells without presenting any specific toxic effect.[16] Whitsitt and co-workers have successfully coated single-walled carbon nanotubes (SWNTs) with pure[17] and fluorine-doped silica[18] with the aid of surfactants using the solution method, which shows retention of the Raman fluorescence properties. In addition, Fu et al. functionalized multiwalled carbon nanotubes (MWCNTs) with $Co_3O_4$ nanospheres, showing that the nanocomposites can possess rectifying diode characteristics.[19]

It is well-known that transition-metal compounds play important roles in nanoscale motifs, which are of great scientific and technological importance in applications such as photonic materials, nanosized reactors, miniaturized sensors, catalytic materials, and novel characteristics due to their high aspect ratios and quantum size effects.[20] Among the inorganic complex family, nickel sulfides are very interesting because of their promising uses as transformation toughening agents for materials applied in the semiconductor industry, catalysts for organic reactions, and coatings for photogalvanic cells.[21] Particularly, the electronic and magnetic properties of $Ni_3S_2$ have attracted more interest, attributed to strong electron−electron correlation effects, magnetic instabilities, and insulating ground states.[22] Moreover, $Ni_3S_2$ also undergoes similar volume-expansion phase transformations upon cooling and may act as a transformation toughener.[23] In this work, we successfully functionalized CNTs with $Ni_3S_2$ nanostructures to grow MWCNTs/$Ni_3S_2$ heterostructures by using the solvent−thermal method. Interestingly, without ammonia in the reaction solution, the nanocomposites show that the outside surfaces of MWCNTs are uniformly coated by a $Ni_3S_2$ film resembling centipede-shaped objects. When the ammonia was added to the reaction solution, keeping all other conditions unvaried, the clustered $Ni_3S$ nanoparticles were formed along the outside surface of the MWCNTs. On the basis of our experimental results, we propose a dynamic-controlled Oswald ripening mechanism to elucidate the formation of the MWCNTs' compositions with centipede-shaped and clustered $Ni_3S_2$ morphologies.

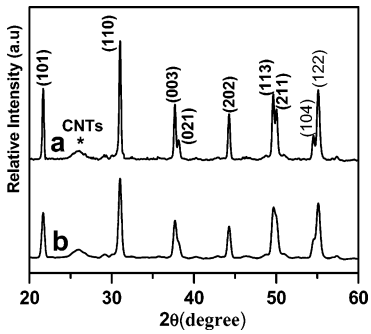


**Figure 1.** XRD spectra of the MWCNTs/$Ni_3S_2$ nanocomposites prepared via treating the reaction precursors solution with 9 mg of MWCNTs, 1.5 mmol of $NiCl_2$, 1 mmol of thiourea, and with (a) or without (b) 1.00 mL of ammonia at 180 °C for 12 h.

## 2. Experimental Section

MWCNTs with a purity of 95% were produced via the catalytic decomposition of $CH_4$.[24] All chemicals were of analytical grade and used without further purification. In a typical experiment to prepare the MWCNTs/$Ni_3S_2$ nanocomposites, 9 mg of MWCNTs, 1.5 mmol of nickel chloride, and 1.0 mmol of thiourea were added to 12 mL of ethanol with and/or without 1.00 mL of ammonia (28%). And the mixture was transferred to a stainless-steel autoclave of 22 mL capacity. After sealing, the autoclave was heated to 180 °C for 12 h and cooled to room temperature under ambient atmosphere, resulting in the formation of the MWCNTs/$Ni_3S_2$ nanocomposites. The resultant samples were washed with deionized water and then with ethanol three times under ultrasonication. The products were then separated by centrifugation at 4000 rpm. Finally, the products were dried at 50 °C in a vacuum oven before further characterization. In order to investigate the influence of the reaction conditions on the sample morphologies, the comparison experiments were carried out under imilar conditions except that the quantity of reaction precursors was changed.

The X-ray diffraction (XRD) patterns of the samples were obtained with a powder X-ray diffractometer (D/Max 2550 V, Rigaku, Japan), using Kα radiation ($\lambda = 1.5418$ Å). The scanning electron microscopy (SEM) images were taken on a JEOL JSM-6700F instrument. Transmission electron microscopy (TEM,) energy-dispersive X-ray spectroscopy (EDS), and selected area electronic diffraction (SAED) tests were performed with a JEM 2010 (JEOL) instrument.

## 3. Results and Discussions

**3.1. X-ray Diffractive Patterns of the Obtained Products.** Representative XRD patterns of the sample obtained by treating the ethanol solution in the presence of 1.5 mmol of $NiCl_2$ and 1.0 mmol of thiourea with or without 1.00 mL of ammonia are shown in parts a and b of Figure 1 respectively. Both samples show similar diffraction patterns, proving the existence of the same crystal phase of both samples. The peaks centered at 26° can be nicely indexed to the (002) plane of CNTs as depicted with the star in Figure

(12) Zhang, W.; Suhr, J.; Koratkar, N. A. *Adv. Mater*. **2006**, *18*, 452.
(13) Zhang, Y.; Liu, C.; Li, F.; Cheng, H. M. *New Carbon Mater*. **2006**, *21*, 307.
(14) Yu, X.; Munge, B.; Patel, V.; Jensen, G.; Bhirde, A.; Gong, J. D.; Kim, S. N.; Gillespie, J.; Gutkind, J. S.; Papadimitrakopoulos, F.; Rusling, J. F. *J. Am. Chem. Soc.* **2006**, *128*, 11199.
(15) Shiba, K. *J. Drug Targeting* **2006**, *14*, 512.
(16) Wu, W.; Wieckowski, S.; Pastorin, G.; Benincasa, M.; Klumpp, C.; Briand, J. P.; Gennaro, R.; Prato, M.; Bianco, A. *Angew. Chem*. **2005**, *44*, 6358.
(17) Whitsitt, E. A.; Barron, A. R. *Nano Lett.* **2003**, *3*, 775.
(18) Whitsitt, E. A.; Moore, V. C.; Smalley, R. E.; Barron, A. R. *J. Mater. Chem.* **2005**, *15*, 4678.
(19) Fu, L.; Liu, Z.; Liu, Y.; Han, B.; Hu, P.; Cao, L.; Zhu, D. *Adv. Mater.* **2005**, *17*, 217.
(20) Qu, L.; Dai, L.; Osawa, E. *J. Am. Chem. Soc.* **2006**, *128*, 5523.
(21) Ghezelbash, A.; Sigman, M. B.; Korgel, B. A. *Nano Lett.* **2004**, *4*, 537.
(22) Yu, S. H.; Yoshimura, M. *Adv. Funct. Mater*. **2002**, *12*, 277.
(23) (a) Grau, J.; Akinc, M. *J. Am. Ceram. Soc*. **1996**, *79*, 1073. (b) Grau, J.; Akinc, M. *J. Am. Ceram. Soc*. **1997**, *80*, 941.
(24) Liang, Q.; Liu, B. C.; Tang, S. H.; Li, Z. J.; Li, Q.; Gao, L. Z.; Zhang, B. L.; Yu, Z. L. *Acta Chim. Sin*. **2000**, *58*, 1336.

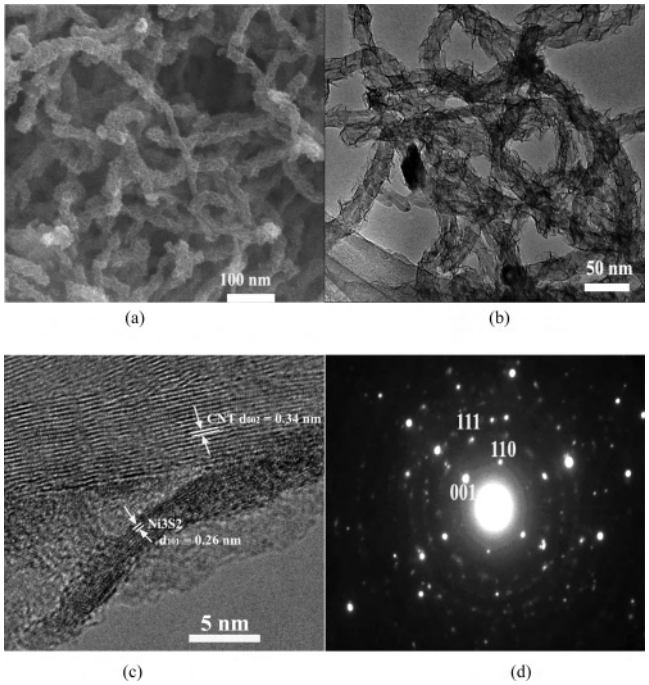


**Figure 2.** (a) SEM, (b) TEM, and (c) HRTEM images and (d) SAED pattern of functionalized MWCNTs with centipede-shaped $Ni_3S_2$ nanostructures.

1a.[25] All the left diffraction peaks can be indexed to the rhombohedral $Ni_3S_2$ with space group *R*32, having cell parameters of $a = 0.4080$ nm and $\alpha = 89.43°$.[22] The EDS spectrum (not shown) confirms that the composite materials are composed of Ni and S, and a quantitative analysis indicates that the Ni/S elemental ratio is 1.46 to 1.1, which agrees well with that from the XRD results.

**3.2. Morphologies of the Obtained Samples.** To ascertain the morphologies of the samples obtained here, the morphologies were characterized by SEM as shown in Figure 2a, indicating that the outside surface of the MWCNTs was uniformly coated by a $Ni_3S_2$ film with lamellar structure. Evidently, the nanocomposites present a rough surface in comparison with that of pristine MWCNTs, verifying that $Ni_3S_2$-functionalized MWCNTs were successfully accomplished in our experiment. As seen from the low-magnification TEM image (Figure 2b), MWCNTs are modified with $Ni_3S_2$ nanostructures located along the outside surface of MWCNTs, whose shape resembles centipede-shaped objects. Moreover, the high-resolution TEM (HRTEM) image clearly shows that the crystalline features of the $Ni_3S_2$ coating are of polycrystalline phase with discontinuous crystal fringes as shown in Figure 2c, whose lattice spacing is about 0.26 nm, corresponding to the (101) crystal plane of $Ni_3S_2$.[26] The (002) lattice plane of the graphitic interlayer of MWCNTs was clearly identified, with the interlayer distance of 0.34 nm as seen in Figure 2c. The SAED patterns were recorded from the centipede-shaped nanocomposites. The diffraction spots can correspond to the (001), (110), and (111) of the rhombohedra $Ni_3S_2$ crystallite with the electron beam along the [001] direction.

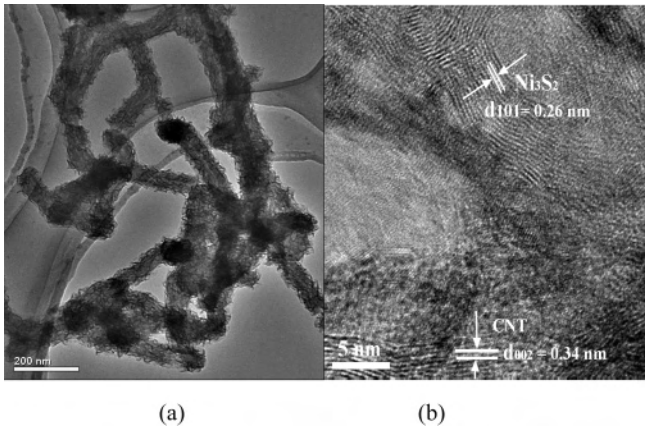


**Figure 3.** (a) TEM and (b) HRTEM images of samples synthesized with 3 mmol of $NiCl_2$ and 2 mmol of thiourea in the ethanol solution, respectively.

To date, the concentration of the reaction precursors can affect the morphologies of nanomaterials.[27] For instance, Loscutova et al. reported controlled synthesis of CdS, CdSe−SWCNTS hybrid nanocompositions by changing the concentration of the SWCNTs and cadmium source.[28] Therefore, our parallel experiments were performed under the same experimental conditions except 3 mmol of $NiCl_2$ and 2 mmol of thiourea were used in the reaction solution. As expected, the $Ni_3S_2$ thin layers were generated along the outer surfaces of MWCNTs with the unsmooth characteristics as shown in Figure 3a. By close observation, the $Ni_3S_2$ layer is thicker than that with 1.5 mmol of $NiCl_2$ and 1 mmol of thiourea, indicating that the layer thickness can be tuned by simply adjusting the reaction precursor concentration while fixing all other reaction conditions. Furthermore, the HRTEM image (Figure 3b) indicates that the lattice fringe with the crystal spacing of 0.26 nm corresponding to the (101) crystal planes is unordered due to its polycrystalline phase.

It is well-known that the controlled synthesis of nanomaterials is very interesting due to some undiscovered properties originating from the different morphologies of the products.[29] Hence, in our experiment, the ammonia was added to try to control the nanocomposite morphology owing to its directing role during the nanomaterial synthetic processes.[30] Surprisingly, when 1.00 mL of ammonia was added to the ethanol solution with 1.5 mmol of $NiCl_2$ and 1 mmol of thiourea under similar experimental conditions, the resultant products showed that MWCNTs are randomly attached with a large quantity of $Ni_3S_2$ nanoparticles, as seen in the SEM image in Figure 4a. The low-magnification TEM image (Figure 4b) also shows that $Ni_3S_2$ nanoparticles with a diameter of about 25 nm were separately coated on the outer surface of MWCNTs. During the synthesis of $Ni_3S_2$ nanoparticles, the

(25) Li, W.; Wang, X.; Chen, Z.; Waje, M.; Yan, Y. *J. Phys. Chem. B* **2006**, *110*, 15353.
(26) Zhang, W.; Xu, L.; Tang, K.; Li, F.; Qian, Y. *Eur. J. Inorg. Chem.* **2005**, 653.
(27) (a) Hu, X. L.; Zhu, Y. J. *Langmuir* **2004**, *20*, 1521. (b) Pileni, M. P. *J. Phys. Chem. C* **2007**, *111*, 9019. (c) Peng, W.; Qu, S.; Cong, G.; Wang, Z. *Cryst. Growth Des.* **2006**, *6*, 1518.
(28) Loscutova, R.; Barron, A. R. *J. Mater. Chem.* **2005**, *15*, 4346.
(29) Zhang, H.; Wang, D.; Mhwald, H. *Angew. Chem.* **2006**, *45*, 748.
(30) Tsuji, M.; Hashimoto, M;. Nishizawa, Y.; Kubokawa, M.; Tsuji, T. *Chem.—Eur. J.* **2005**, *11*, 440.

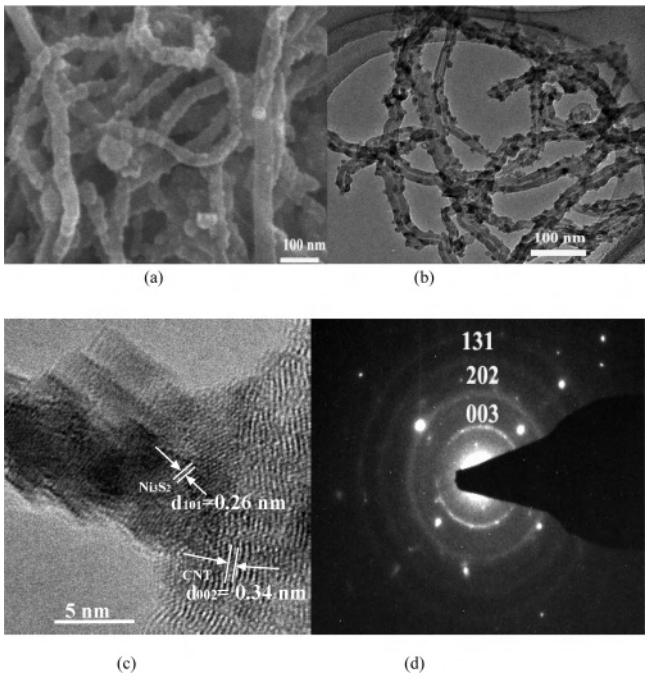


**Figure 4.** (a) SEM, (b) TEM, (c) and HRTEM images and (d) SAED pattern of nanoparticle $Ni_3S_2$-coated MWCNTs synthesized with 1.00 mL of ammonia in the reaction solution.

MWCNTs can act as a template, which limits the produced $Ni_3S_2$ particles access to one another, thereby forming quasi-one-dimensional $Ni_3S_2$ nanoparticles along the MWCNTs outside surface. The detailed microstructure information of the $Ni_3S_2$ nanoparticles is further characterized by HRTEM (Figure 4c), which shows $Ni_3S_2$ nanoparticles lattice fringes of 0.26 nm ascribed to (101) lattice spacing of the rhombohedra structure $Ni_3S_2$. By careful analysis, it was evident that the typical HRTEM image shows that the $Ni_3S_2$ nanoparticles have disorderly stacking faults in a vertical orientation to the MWCNTs surface, resulting from the poor crystal quality. The SAED patterns (Figure 4d) show diffraction rings, indicating that the produced $Ni_3S_2$ nanoparticles are polycrystalline. The two inside track diffraction rings correspond to (003), (202), and (131) reflections of rhombohedra $Ni_3S_2$ phase, respectively, which are in good agreement with the XRD data described above.

To investigate the influence of ammonia concentration on the morphology of the samples, the controlled experiments were conducted with 0.50 and 3.00 mL of ammonia, respectively, while keeping the other conditions unchanged. The synthesized products exhibit similar morphologies similar to those mentioned above, as seen in the TEM images shown in Figure 5. In particular, the TEM image (Figure 5a) reveals that $N_3S_2$ nanoparticles with a size of 12 nm synthesized with 0.50 mL of ammonia were attached to the outside surface of the MWCNTs. The HRTEM (Figure 5b) image provides further microstructure of the obtained samples, verifying that $Ni_3S_2$ nanoparticles are stacking on the outer surfaces of CNTs with a lattice spacing of about 0.26 nm corresponding to the (101) crystal plane. In addition, it also demonstrates the graphite layer distance of approximately 0.34 nm for the (002) graphite layers. However, when the amount of ammonia added was increased to 3.00 mL, $Ni_3S_2$ particles with the large size of about 80 nm adhered to the outer surfaces of MWCNTs, as shown in Figure 5c. Further, the HRTEM image (Figure 5d) reveals that $Ni_3S_2$ nanoparticles display crossing features owing to assembly of the small particles during the reaction processes. Meanwhile, the $Ni_3S_2$ nanopartices have polycrystalline characteristics with a lattice spacing of 0.26 nm for its (101) crystal plane. These observations suggest that particle nucleation and growth should be correlated with ammonia coordination with nickel ions in the reaction solution.

**3.3. Possible Formation Mechanism of Nanocomposites.** On the basis of our experimental results, MWCNTs were functionalized with metallic $Ni_3S_2$ nanostructures with heat treatment of the reaction precursors in ethanol solution with and/or without ammonia at 180 °C for 12 h. In the absence of ammonia, the $Ni_3S_2$ structure which was coated on the outside surface of MWCNTS shows the centipede-shaped structures. Interestingly, in the presence of ammonia, $Ni_3S_2$ nanoparticles were formed along the outside surface of MWCNTS. Furthermore, the sizes of $Ni_3S_2$ nanoparticles can be tuned via the addition of different amounts of ammonia under the same reaction conditions. On the basis of these facts, we propose the dynamic-controlled growth mechanism to account for the MWCNTs/$Ni_3S_2$ nanocomposites as follows:

$$\mathrm{EtOH} \leftrightarrow \mathrm{H^{\bullet}} + \mathrm{EtO^{\bullet}} \quad (1)$$

$$2\mathrm{H^{\bullet}} + \mathrm{RS} \rightarrow \mathrm{H_2S} + \mathrm{R^{\bullet}}\ (\mathrm{RS} = \mathrm{H_2NCSNH_2}) \quad (2)$$

$$\mathrm{S^{2-}} + \mathrm{Ni^{2+}} \rightarrow (\mathrm{NiS})n \quad (3)$$

$$n(\mathrm{NiS}) + \mathrm{MWCNTs} \rightarrow \mathrm{MWCNTs/Ni_3S_2} \quad (4)$$

Equation 1 represents the radicals ($H^{\bullet}$ and $EtO^{\bullet}$)) from ethanol once the solution is treated at high temperature.[31] Equations 2−4 represent the main reactions leading to the formation of $Ni_3S_2$ clusters in solution by heat treatment. From the the low-energy viewpoint, the initially generated $Ni_3S_2$ nuclei may attach on the surface of the MWCNTs to form small $Ni_3S_2$ crystal nuclei. In the absence of ammonia in the solution, $Ni_3S_2$ crystal nuclei can rapidly grow and coat the outside surface of MWCNTs to form layered structures with characteristics similar to those of polymers. Then, the layered structures of $Ni_3S_2$-coated MWCNTS can grow some legs with acentipede-like shape due to the active growth of the $Ni_3S_2$ (101) crystal plane compared with the other crystal planes when heating the reaction solution. When adding ammonia to the mixture solution, the Ni ions must be coordinated with ammonia to become $Ni(NH_3)n^{2+}$. Due to the low speed of the Ni ions dissolution from $Ni(NH_3)$-$n^{2+}$, the produced $Ni_3S_2$ nuclei on the outside surface of the MWCNTs must proceed at a slower speed when compared with that in the absence of ammonia and grow into big particles via an Oswald formation mechanism. The more ammonia, the slower the speed of the growth of $Ni_3S_2$ due to the ammonia-coordinated function with indium ions and

(31) Gao, T.; Wang, T. *Chem. Commun*. **2004**, 2558.

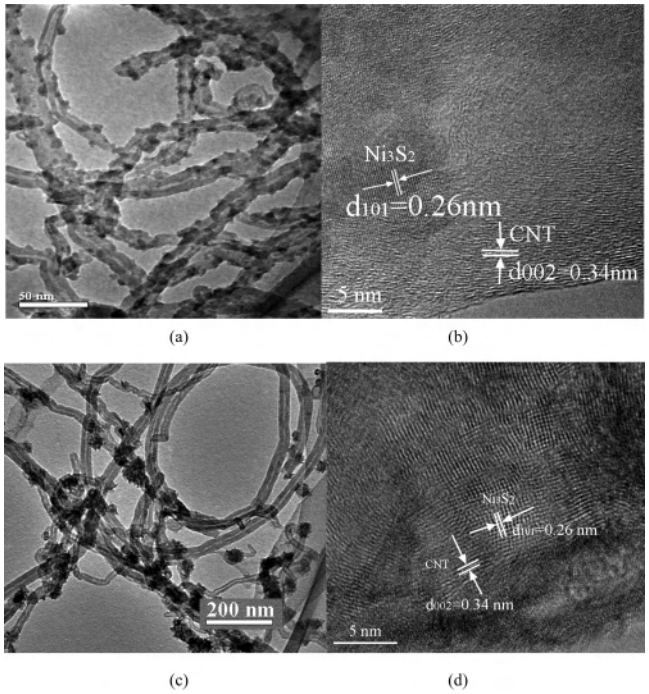


**Figure 5.** (a and c) TEM and (b and d) HRTEM images of MWCNTs functionalized with nanoparticle $Ni_3S_2$ prepared with 0.50 and 3.00 mL of ammonia, while the other reaction conditions remain unchanged.

the larger the size of the $Ni_3S_2$ nanoparticles on the outside surface of the MWCNTs.

## 4. Conclusions

In summary, the functionalization of MWCNTs with different motifs of $Ni_3S_2$ nanomaterials was successfully achieved using the facile hydrothermal route. Furthermore, the morphologies of $Ni_3S_2$-coated MWCNTs can be tuned from centipede-shaped motifs to nanoparticles when 1 mL of ammonia is added to the reaction system while keeping the other conditions unchanged. On the basis of the previously reported literature and our experimental results, it is proposed that a dynamic-controlled Oswald ripening mechanism was responsible for the formation of the different profiles of the obtained products. We claim that the facile method can readily be applied to synthesize other transition-metal sulfides with the appropriate precursors. Moreover, the MWCNTs/$Ni_3S_2$ materials can supply a platform to investigate their potential applications as nanoscale optical-electronic devices.

**Acknowledgment.** This work was supported in part by the Korea Research Foundation Grant funded by the Korean Government (MOEHRD) (KRF-2005-005-J11903) and also, in part, by the SRC program (Center for Nanotubes and Nanostructured Composites) of the Ministry of Science and Technology of the Korea/Korea Science and Engineering Foundation.

**Supporting Information Available:** UV−vis absorption spectra of the samples dispersed in ethanol recorded on a TU-1201 spectrophotometer; results of quantum calculations performed using density functional theory with CASTEP code. This material is available free of charge via the Internet at http://pubs.acs.org.

IC700936C